

2-26-2008

Dynamic Solvation in Phosphonium Ionic Liquids: Comparison of Bulk and Micellar Systems and Considerations for the Construction of the Solvation Correlation Function, $C(t)$

Prasun Mukherjee
Iowa State University

Jeffrey Aaron Crank
University of Texas, jeffreycrank@gmail.com

Pritesh S. Sharma
University of Texas

Aruna B. Wijeratne
University of Texas

Follow this article and additional works at: http://lib.dr.iastate.edu/chem_pubs



Part of the [Biochemistry Commons](#), and the [Chemistry Commons](#)

See next page for additional authors.

The complete bibliographic information for this item can be found at http://lib.dr.iastate.edu/chem_pubs/563. For information on how to cite this item, please visit <http://lib.dr.iastate.edu/howtocite.html>.

Dynamic Solvation in Phosphonium Ionic Liquids: Comparison of Bulk and Micellar Systems and Considerations for the Construction of the Solvation Correlation Function, $C(t)$

Abstract

Dynamic solvation of the dye coumarin 153 is studied in a phosphonium ionic liquid: hexadecyltributylphosphonium bromide, $[(C4)3C16P^+][Br^-]$. It forms micelles in water, and the bulk also exists as a liquid under our experimental conditions. This system permits a comparison with an imidazolium ionic liquid studied earlier, which also formed micelles in water (*J. Phys. Chem. A* **2006**, *110*, 10725–10730). We conclude that our analysis of the comparable situation in a phosphonium liquid is not as definitive as we had proposed earlier, i.e., that the majority of the early-time solvation arises from the organic cation. Part of the difficulty in performing this analysis is most likely due to the amount of water that is associated with the micelle. In the course of this work, we have focused on the calculation of the solvation correlation function, $C(t)$, and investigated how it depends upon the methods with which the “zero-time” spectrum is constructed.

Keywords

Correlation methods, fluids, ionization of liquids, solvation, Coumarin 153, micellar system

Disciplines

Biochemistry | Chemistry

Comments

Reprinted (adapted) with permission from *Journal of Physical Chemistry B* 112 (2008): 3390, doi: [10.1021/jp7107126](https://doi.org/10.1021/jp7107126). Copyright 2008 American Chemical Society.

Authors

Prasun Mukherjee, Jeffrey Aaron Crank, Pritesh S. Sharma, Aruna B. Wijeratne, Ramkrishna Adhikary, Sayantan Bose, Daniel W. Armstrong, and Jacob W. Petrich

Dynamic Solvation in Phosphonium Ionic Liquids: Comparison of Bulk and Micellar Systems and Considerations for the Construction of the Solvation Correlation Function, $C(t)$

Prasun Mukherjee,[†] Jeffrey A. Crank,[‡] Pritesh S. Sharma,[‡] Aruna B. Wijeratne,[‡] Ramkrishna Adhikary,[†] Sayantan Bose,[†] Daniel W. Armstrong,[‡] and Jacob W. Petrich^{*†}

Department of Chemistry, Iowa State University, Ames, Iowa 50011, and Department of Chemistry and Biochemistry, University of Texas, Arlington, Box 19065, Arlington, Texas 76019

Received: November 8, 2007; In Final Form: December 7, 2007

Dynamic solvation of the dye coumarin 153 is studied in a phosphonium ionic liquid: hexadecyltributylphosphonium bromide, $[(C_4)_3C_{16}P^+][Br^-]$. It forms micelles in water, and the bulk also exists as a liquid under our experimental conditions. This system permits a comparison with an imidazolium ionic liquid studied earlier, which also formed micelles in water (*J. Phys. Chem. A* 2006, 110, 10725–10730). We conclude that our analysis of the comparable situation in a phosphonium liquid is not as definitive as we had proposed earlier, i.e., that the majority of the early-time solvation arises from the organic cation. Part of the difficulty in performing this analysis is most likely due to the amount of water that is associated with the micelle. In the course of this work, we have focused on the calculation of the solvation correlation function, $C(t)$, and investigated how it depends upon the methods with which the “zero-time” spectrum is constructed.

Introduction

Room-temperature ionic liquids, most commonly comprised of organic cations and inorganic anions, are receiving an increasing amount of attention because of their utility as environmentally friendly, “green” solvents and because of a host of practical applications to which they are amenable.^{1–4} The importance of ionic liquids has consequently stimulated considerable interest in their dynamic solvation properties.^{5–34} A special issue of *The Journal of Physical Chemistry* has recently been devoted to ionic liquids.³⁵ Major questions regarding dynamic solvation by ionic liquids deal with whether the organic cation or the inorganic anion solvates preferentially on different time scales, the role of the correlated motion of the ion pairs and their lifetime, and the importance of translational motion of the ions relative to dipolar relaxation.^{23–25} Previously, we attempted to address some of these questions by studying the solvation of the dye coumarin 153 in a bulk imidazolium ionic liquid, 1-cetyl-3-vinylimidazolium bromide $[(CVIM^+)[Br^-]]$, and its corresponding micelle in water.³⁶ (There is a growing body of work on the subject of ionic liquids in micelles, microemulsions, and related systems.^{37–43}) Because coumarin 153 is only sparingly soluble and weakly fluorescent in water, a clear distinction can be made between its fluorescent properties in the bulk ionic liquid and those in the micelles formed from the ionic liquid. We concluded from this study that the same entity is responsible for the majority of the solvation in both the bulk and micellar $[CVIM^+][Br^-]$ ionic liquid, namely, as we have suggested elsewhere,^{23–25} that it is the imidazolium cation. This study was, however, limited: first, because bulk $[CVIM^+][Br^-]$ could only be studied as an opaque solid at the temperatures at which we investigated the micelle; second, because the study only considered ionic liquids based upon imidazolium. In this work, we investigate a phosphonium ionic liquid (Figure 1), which forms micelles in water and for which

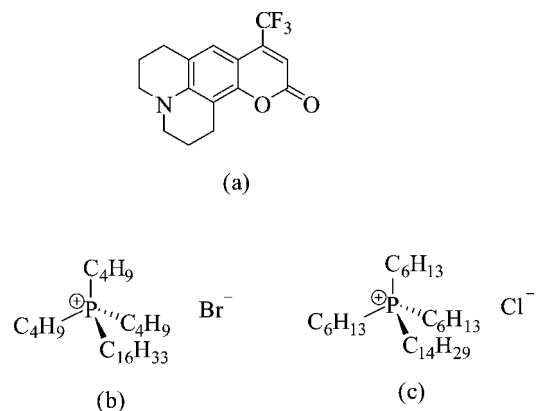


Figure 1. Structures of the solvation probe (a) coumarin 153 (C153) and the two ionic liquids studied in this work: (b) hexadecyltributylphosphonium bromide $[(C_4)_3C_{16}P^+][Br^-]$, melting point 58–60 °C, and (c) tetradecyltriethylphosphonium chloride $[(C_2)_3C_{14}P^+][Cl^-]$ (liquid at room temperature). $[(C_4)_3C_{16}P^+][Br^-]$ forms micelles in water.

the bulk also exists as a liquid under our experimental conditions: hexadecyltributylphosphonium bromide, $[(C_4)_3C_{16}P^+][Br^-]$ (melting point of 58–60 °C). As a result of this study, our earlier conclusions have been tempered, and most importantly, we present conclusions dealing with the construction of the solvation correlation function, $C(t)$.

Materials and Methods

Preparation and Purification/Decolorization of Low-Melting-Point Phosphonium Halide Organic Salts. Phosphonium halide ionic liquids (ILs) were donated by Cytec Inc. and were decolorized according to the procedure described elsewhere.⁴⁴ A conventional column used for flash chromatography was packed with the following compounds: Celite on the bottom to trap charcoal particles, flash chromatographic silica gel and alumina in the middle for decolorization and removal of polar and inorganic impurities, and charcoal on the top for decolorizing. The column was treated with dichloromethane (CH_2Cl_2)

* To whom correspondence should be addressed.

[†] Iowa State University.

[‡] University of Texas.

(3 × 200 mL). The room temperature IL (RTIL) was dissolved in CH₂Cl₂ (200 mL) and passed through the column. Then CH₂Cl₂ (200 mL) was passed to elute the remainder of the ionic liquid. To purge the ionic liquid through the column, N₂ gas was passed over the column. To obtain some visible change in color during the decolorization, the aforementioned procedure (the passage of the RTIL dissolved in CH₂Cl₂) was repeated more than 15 times. Also, during each of the repetitions, the column was treated with CH₂Cl₂ (200 mL). The eluted solution was then concentrated under reduced pressure and finally by heating at 60 °C in vacuo overnight. Structures were verified by ¹H NMR and ESI-MS. The water contents of the RTILs were measured by coulometric Karl Fischer titration (Mettler Toledo DL 39).

CMC Determination. The critical micelle concentration (CMC) was found by plotting surface tension (dyn/cm) vs concentration (M). Surface tension measurements were taken using a Fischer model 20 surface tensiometer. All glassware used was cleaned by chromic acid, rinsed with deionized water, and dried in an oven. Concentrations of hexadecyltributylphosphonium bromide between 0 and 0.1 M were prepared in aqueous solution at room temperature. An average of three measurements was taken to represent the surface tension at each concentration of IL. The CMC value of the [(C₄)₃C₁₆P⁺][Br⁻] micelle was found to be 2 × 10⁻³ M at room temperature.

Determination of the Micellar Aggregation Number. The aggregation number (the average number of surfactant molecules per micelle) can be estimated by optical techniques proposed by Turro and Yekta⁴⁵ and later modified by De Schryver and co-workers.⁴⁶ As before,³⁶ we employ the latter method, where the micellar aggregation number is obtained by exploiting the vibronic fine structure of pyrene emission. Pyrene was recrystallized several times from absolute ethanol before use. Three stock solutions were prepared of pyrene in ethanol, cetylpyridinium chloride in water, and [(C₄)₃C₁₆P⁺][Br⁻] in water at concentrations of 2 × 10⁻⁴, 10 × 10⁻³, and 5 × 10⁻² M. For all measurements, pyrene and surfactant concentrations were kept constant at ~2 × 10⁻⁶ and ~2 × 10⁻² M. Six solutions were prepared with increasing quencher concentration from 0 to 0.5 × 10⁻³ M. Samples were excited at 337 nm. The aggregation number was determined by the same procedure we have employed elsewhere. Calculations can be performed using the intensity of either band I or band III of pyrene emission. We have chosen the emission intensity of band I (at ~373 nm) and band III (at ~384 nm) for determining the aggregation number of the micelle. The results obtained from both bands were identical. The mean aggregation number of the [(C₄)₃C₁₆P⁺][Br⁻] micelle at room temperature was found to be 40.

Preparation of Micellar Solutions. The cmc of [(C₄)₃C₁₆P⁺][Br⁻] in water was found to be 2 × 10⁻³ M at 22 °C; see above. For all experiments in micellar systems, the C153 concentration was kept at ~6 × 10⁻⁶ M in ~2 × 10⁻² M [(C₄)₃C₁₆P⁺][Br⁻] (10(CMC)), and a ~3330:1 surfactant-to-C153 ratio was maintained. Under these conditions there is one C153 molecule for every 75 micelles, thus minimizing the possibility of aggregation.

Preparation of Solutions for Stern–Volmer Quenching Experiments. We initially attempted to perform quenching experiments with iodide anion, as we did in our previous work. We were not able to attain concentrations of I⁻ higher than 3 mM due to solubility problems and consequently were not able to obtain enough data to determine quenching constants. We thus opted for *N,N*-dimethylaniline (DMA) to quench C153 fluorescence in this system. For quenching of C153 in bulk

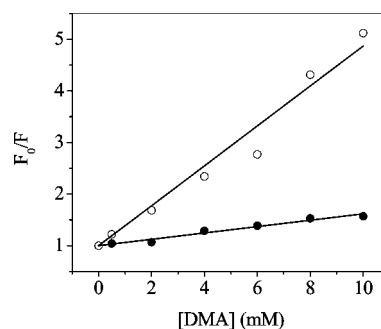


Figure 2. Stern–Volmer quenching plots of C153 by DMA in acetonitrile (solid circles) and [(C₄)₃C₁₆P⁺][Br⁻] micelles (open circles). *K_{SV}* values were found to be 60 M⁻¹ for C153 in acetonitrile and 390 M⁻¹ for the [(C₄)₃C₁₆P⁺][Br⁻] micelle. All experiments were done at room temperature. DMA is negligibly soluble in water, and on the basis of NMR⁶⁷ and fluorescence⁶⁸ measurements in CTAB micelles, it has been concluded that DMA resides in the head group region of the micelles. We expect the same location of DMA in [(C₄)₃C₁₆P⁺][Br⁻] micelles. The very efficient quenching of C153 fluorescence by DMA (most likely by electron transfer from DMA to C153)^{69,70} indicates that the probe molecules are accessible to the quencher.

solvent, a stock solution of 2 × 10⁻⁴ M C153 in acetonitrile was used. The corresponding quenching experiment in micellar environment was performed by preparing two stock solutions: 2 × 10⁻⁴ M C153 in acetonitrile and 5 × 10⁻² M [(C₄)₃C₁₆P⁺][Br⁻] in water. For all measurements, the C153 and surfactant concentrations were kept constant at ~2 × 10⁻⁶ and ~5 × 10⁻³ M (2.5(CMC)), and an 830:1 surfactant-to-C153 ratio was maintained. Under these conditions there is one C153 molecule for every 18 micelles, thus minimizing the possibility of aggregation. Seven solutions were prepared with increasing quencher concentration from 0 to 10 × 10⁻³ M. We could not increase the quencher concentration above 10 × 10⁻³ M due to precipitation of the surfactant at higher DMA concentration. Emission spectra were obtained using an excitation wavelength of 420 nm. The control experiment was performed in acetonitrile rather than in bulk [(C₄)₃C₁₆P⁺][Br⁻] owing to the difficulties imposed in preparing solutions by the high viscosity of the bulk and the rather small quantities available to us of the purified material.

Steady-State Optical Measurements. Steady-state excitation and emission spectra were recorded with a SPEX Fluoromax-2 with a 2 nm band-pass and were corrected for detector response. A 1 cm path length quartz cuvette was used for the measurements. During spectroscopic measurements, the quartz cuvettes were kept tightly sealed to prevent moisture from being absorbed by the ionic liquids. The steady-state spectra can be used to compute the reorganization energy, λ :²⁴

$$\lambda = \hbar \frac{\int_0^\infty d\nu [\sigma_a(\nu) - \sigma_f(\nu)] \nu}{\int_0^\infty d\nu [\sigma_a(\nu) + \sigma_f(\nu)]} \quad (1)$$

$\sigma_{a,f}$ are the absorption (or excitation) and emission spectral line-shapes, respectively.

Time-Resolved Measurements. The apparatus for the time-correlated single-photon counting measurements is described in detail elsewhere.²³ The instrument response function had a full width at half-maximum (fwhm) of ≤100 ps. A 1 cm path length quartz cuvette was used for all the time-resolved measurements. To construct the time-resolved spectra, a series of decays (~3000 counts in the peak channel for the data presented here, i.e., the 4 and 20 ns full-scale windows) were collected over as much of the fluorescence spectrum as possible,

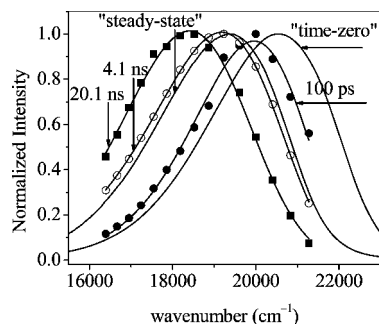


Figure 3. Time-resolved fluorescence emission spectra of C153 in bulk $[(C_4)_3C_{16}P^+][Br^-]$ (66 °C) at 100 ps, 4.1 ns, and 20.1 ns. Corresponding steady-state and time-zero spectra are also included. Note that the 4.1 and 20.1 ns spectra cross the steady-state spectrum, indicating that this spectrum does not adequately report on the completed solvation of C153, as would usually be expected.

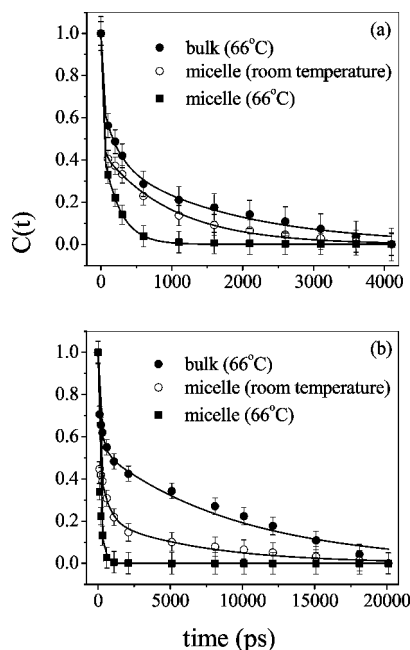


Figure 4. $C(t)$ curves for C153 in (a) bulk $[(C_4)_3C_{16}P^+][Br^-]$ (66 °C) (solid circles) [$C(t) = 0.30 \exp(-t/0.63 \text{ ps}) + 0.29 \exp(-t/210 \text{ ps}) + 0.41 \exp(-t/1730 \text{ ps})$], $[(C_4)_3C_{16}P^+][Br^-]$ under micellar conditions at room temperature (open circles) [$C(t) = 0.56 \exp(-t/20 \text{ ps}) + 0.44 \exp(-t/1000 \text{ ps})$], at 66 °C (solid squares) [$C(t) = 0.48 \exp(-t/0.35 \text{ ps}) + 0.52 \exp(-t/230 \text{ ps})$], with a time window of 4 ns and (b) bulk $[(C_4)_3C_{16}P^+][Br^-]$ (66 °C) (solid circles) [$C(t) = 0.22 \exp(-t/2.5 \text{ ps}) + 0.24 \exp(-t/300 \text{ ps}) + 0.54 \exp(-t/9700 \text{ ps})$], $[(C_4)_3C_{16}P^+][Br^-]$ under micellar conditions at room temperature (open circles) [$C(t) = 0.49 \exp(-t/1.3 \text{ ps}) + 0.30 \exp(-t/590 \text{ ps}) + 0.21 \exp(-t/7000 \text{ ps})$] and at 66 °C (solid squares) [$C(t) = 0.45 \exp(-t/0.13 \text{ ps}) + 0.55 \exp(-t/210 \text{ ps})$], with a time window of 20 ns. In all cases the initial fast component occurs within our instrumental time resolution. Most importantly, there is a dependence of $f_{100\text{ps}}$ and the average solvation time on the choice of the time scale of the experiment for the bulk $[(C_4)_3C_{16}P^+][Br^-]$ (66 °C) and $[(C_4)_3C_{16}P^+][Br^-]$ under micellar conditions at room temperature. This effect is more pronounced in the bulk compared to that in the micellar system. However, no such effect was observed for $[(C_4)_3C_{16}P^+][Br^-]$ under micellar conditions at 66 °C on changing the time scale from 4 to 20 ns, indicating faster solvation in this system.

typically from 470 to 610 nm at 10 nm intervals. They were fit to a maximum of three exponentials. Transient spectra were reconstructed from these fits in the standard manner.^{23,36} We have employed the traditional approach of fitting the time-resolved spectra to a log-normal function, from which we extract the peak frequency, $\nu(t)$, as a function of time.

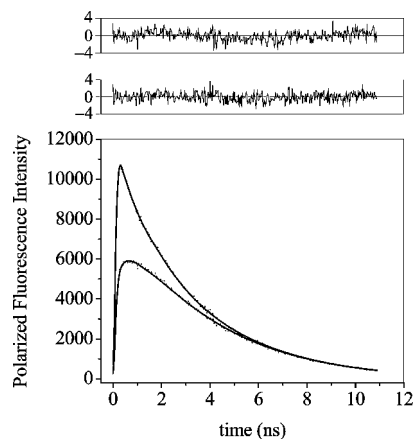


Figure 5. Representative polarized fluorescence decay of C153 in $[(C_4)_3C_{16}P^+][Br^-]$ under micellar conditions at room temperature. Fitting parameters are given in Table 2.

The solvation dynamics were described by the normalized correlation function

$$C(t) = \frac{\nu(t) - \nu("∞")}{\nu("t = 0") - \nu("∞")} \quad (2)$$

$\nu("t = 0")$ is the frequency at "zero-time", as calculated by the method of Fee and Maroncelli.⁴⁷ $\nu("∞")$ is the frequency at "infinite time", which may be taken as the maximum of the steady-state fluorescence spectrum if solvation is more rapid than the population decay of the probe. $\nu(t)$ is determined by taking the maxima from the log-normal fits as the emission maximum. In most of the cases, however, the spectra are broad, so there is some uncertainty in the exact position of the emission maxima. Thus, we have considered the range of the raw data points in the neighborhood of the maximum to estimate an error for the maximum obtained from the log-normal fit. Depending on the width of the spectrum (i.e., zero-time, steady-state, or time-resolved emission spectrum), we have determined the typical uncertainties as follows: zero-time \approx steady-state ($\sim \pm 100 \text{ cm}^{-1}$) < time-resolved ($\sim \pm 200 \text{ cm}^{-1}$) emission. We use these uncertainties to compute error bars for $C(t)$. Finally, in generating $C(t)$, the first point was obtained from the zero-time spectrum. The second point was taken at the maximum of the instrument response function, which, having a full width at half-maximum of $\leq 100 \text{ ps}$, was taken to be $\sim 100 \text{ ps}$. Fractional solvation at 100 ps was calculated using $f(t = 100 \text{ ps}) = 1 - C(t = 100 \text{ ps})$.

Results

C153 is sparingly soluble in water and hence must be located in the micelles formed by $[(C_4)_3C_{16}P^+][Br^-]$. To characterize its location therein, we constructed Stern-Volmer plots using DMA as a quencher. Figure 2 presents the Stern-Volmer plots of C153 quenched by DMA in acetonitrile and micelles formed by $[(C_4)_3C_{16}P^+][Br^-]$. K_{SV} values were 60 M^{-1} for C153 in acetonitrile and 390 M^{-1} for the $[(C_4)_3C_{16}P^+][Br^-]$ micelle. The greater K_{SV} value in the micelle compared to that in the bulk might be attributed to greater accessibility of C153 to the quencher in the micelle. We suppose this is due to the close proximity of C153 and DMA, the latter being preferentially located in the Stern layer of the micelle. This situation is comparable to that of $[CVIM^+][Br^-]$, where C153 is quenched more efficiently in the micelle than in the bulk reference solvent.³⁶ In both cases, C153 is interpreted to be located in

TABLE 1: Solvation of Coumarin 153 in Bulk and Micellar Phosphonium Ionic Liquid Systems^a

system	η (cP)	H ₂ O (wt %)	$\lambda_{t=0}^b$ (cm ⁻¹)	λ_{SS}^b (cm ⁻¹)	4 ns window			20 ns window		
					f_{100ps}	$\langle\tau\rangle$ (ns)	$\nu^{("∞")}$ (cm ⁻¹)	f_{100ps}	$\langle\tau\rangle$ (ns)	$\nu^{("∞")}$ (cm ⁻¹)
[(C ₄) ₃ C ₁₆ P ⁺][Br ⁻] bulk (66 °C)	268 ± 2	0.2	1920	2480	0.44 ± 0.06	0.77	19 180	0.29 ± 0.04	5.3	18 410
[(C ₄) ₃ C ₁₆ P ⁺][Br ⁻] micelle (room temp)	1.11 ± 0.01		1980	2740	0.59 ± 0.04	0.45	18 080	0.55 ± 0.04	1.6	17 840
[(C ₄) ₃ C ₁₆ P ⁺][Br ⁻] micelle (66 °C)	0.44 ± 0.01		1920	2660	0.67 ± 0.04	0.12	18 130	0.66 ± 0.04	0.12	18 130
[(C ₆) ₃ C ₁₄ P ⁺][Cl ⁻] bulk (purified) (58 °C)	80 ± 1	0.3	1970	2660	0.41 ± 0.05	0.70	19 160	0.33 ± 0.04	3.9	18 610
[(C ₆) ₃ C ₁₄ P ⁺][Cl ⁻] bulk (unpurified) (58 °C)	234 ± 2	0.3	1960	2460				0.34 ± 0.05	4.9	18 900
[(C ₆) ₃ C ₁₄ P ⁺][Cl ⁻] bulk (58 °C) ^c	230 ^d	0.1	1960	2930				0.03	6.7 ± 1.7	18 540

^a The solvation relaxation functions, $C(t)$, are fit to a sum of two or three exponentially decaying functions, where we attribute no particular physical significance to the choice of the functional form employed. The average solvation time $\langle\tau\rangle$ is calculated as $\langle\tau\rangle = \sum a_i \tau_i$, where a_i are the amplitudes of the exponential functions normalized to sum to unity. $C(t)$ is fit from its value at unity, i.e., starting at " $t = 0$ "; consequently, the early part of its decay is determined by only two points, and $\langle\tau\rangle$ that we report must be considered an upper limit. The fractional solvation at 100 ps is defined in the text and elsewhere.^{24,36} ^b The reorganization energies calculated using eq 1 from either the zero-time spectrum ($t = 0$), obtained using the method of Fee and Maroncelli,⁴⁷ or from the equilibrium spectrum (SS). ^c Reference 11. ^d Reference 66.

TABLE 2: Fluorescence Anisotropy of C153 in Bulk Solvent and Micellar Systems^a

system	r_0	r_1	$\tau^{(r)1}$ (ps)	r_2	$\tau^{(r)2}$ (ps)	$\langle\tau^{(r)}\rangle$ (ps)
[(C ₄) ₃ C ₁₆ P ⁺][Br ⁻] bulk (66 °C)	0.22 ± 0.02	0.09 ± 0.01	260 ± 70	0.13 ± 0.02	3000 ± 400	1900 ± 600
[(C ₄) ₃ C ₁₆ P ⁺][Br ⁻] micelle (room temperature)	0.35 ± 0.03	0.15 ± 0.02	200 ± 80	0.20 ± 0.02	1700 ± 400	1100 ± 500
[(C ₄) ₃ C ₁₆ P ⁺][Br ⁻] micelle (66 °C)	0.25 ± 0.04	0.25 ± 0.04	360 ± 80			360 ± 80

^a The errors are based on the average of three measurements. Fluorescence anisotropy decays are fit to the form $r_0 = r_1 \exp(-t/\tau^{(r)1}) + r_2 \exp(-t/\tau^{(r)2})$. In all cases $\chi^2 \leq 1.3$. All experiments were done on a time scale of 12 ns.

the Stern layer, in proximity to the cation, and exposed to water molecules hydrating the micelle.

Time-resolved spectra are presented in Figure 3 for C153 in bulk [(C₄)₃C₁₆P⁺][Br⁻] at 100 ps, 4 ns, and 20 ns. The corresponding "steady-state" and "time-zero" spectra are also included. Note that the 4 and 20 ns spectra cross the steady-state spectrum, indicating that this spectrum does not adequately report on the completed solvation of C153, as would usually be expected.

Figure 4 illustrates this phenomenon more extensively by presenting the solvation relaxation or correlation functions, $C(t)$, for bulk [(C₄)₃C₁₆P⁺][Br⁻] (66 °C) and [(C₄)₃C₁₆P⁺][Br⁻] under micellar conditions (at room temperature and 66 °C) for increasingly larger time windows: 4 and 20 ns. Relevant spectral parameters are summarized in Table 1. A salient feature is that the fraction of rapid solvation and the average solvation time decrease and increase, respectively, as the time window of the experiment is increased. This phenomenon is intimately related to the fact, which has been mentioned above and noticed elsewhere for related systems,^{10,11} that the spectrum at a given time may be more red-shifted than the "equilibrium" spectrum. We see this clearly in the comparison of the 4 ns, 20 ns, and equilibrium spectra of Figure 3. (We attempted to construct $C(t)$ on an 80 ns time scale as well. The 80 ns spectrum we obtained was red of the 20 ns spectrum, but since the number of counts at 80 ns was so limited, <10, we do not take this result to be quantitative.)

Fluorescence anisotropy decay parameters for bulk [(C₄)₃C₁₆P⁺][Br⁻] and for its micelles in water are presented in Table 2. Figure 5 presents the polarized fluorescence decays for [(C₄)₃C₁₆P⁺][Br⁻] under micellar conditions at room temperature. The fluorescence anisotropy decay parameters of the room-temperature micellar system are comparable to those of the bulk ionic liquid. Nonetheless, the fractional solvation at 100 ps, f_{100ps} , of the former is 0.5, whereas that of the latter is 0.3 (as measured with a 20 ns window). The difference in fractional solvation between the bulk and micellar forms of the phosphonium ionic liquid is considerably larger than that for the imidazolium ionic liquid we investigated earlier, which was within about 10%.

Discussion

Bulk Solvent versus Micellar System. As indicated directly above, there are significant differences between the fractional solvation at early times for the bulk and micellar forms of [(C₄)₃C₁₆P⁺][Br⁻]. In addition, the average solvation time of the bulk at 66 °C is at least 3 times as long as that in the micellar environment at room temperature on the 20 ns time scale (Table 1). The enhanced f_{100ps} in micelles is most likely a result of aqueous solvation. As in the case of the imidazolium ionic liquid,³⁶ quenching experiments indicate that it is likely that C153 resides in the Stern layer of the [(C₄)₃C₁₆P⁺][Br⁻] micelle. Such a probe location can also explain why the average solvation time is considerably longer in bulk [(C₄)₃C₁₆P⁺][Br⁻] compared to that of the micelle. In bulk water, solvation is essentially complete after 1 ps,^{48,49} but water in confined environments gives rise to slower solvation response,^{49,50} which has been argued to arise from a dynamic equilibrium between bound and free water molecules.^{51–56} (We do not, however, subscribe to the idea of "biological water", which some of these latter references argue for.⁵⁷) Consequently, we suggest that the water responsible for the relatively rapid solvation response in the micelles is colocalized in the Stern layer with C153.

It is well to note that temperature can have rather profound effects on the structure of micelles and, consequently, the solvation dynamics at their interfaces. The temperature dependence of the structure and hydration number of Triton X-100 (TX-100) micelles was demonstrated by Streletsky and Phillips,⁵⁸ who reported an increase in the hydration number of the micelle with an increase in temperature. The temperature dependence of the solvation dynamics in micelles was studied in TX-100 using 4-aminophthalimide (4-AP) as a fluorescent probe, where an increase in temperature from 283 to 323 K results in a ~8-fold decrease in the average solvation time. From this study the authors also concluded that a temperature-dependent change of the structure and hydration number in the TX-100 micelle appears to play a minor role in their measurements of solvation dynamics.⁵⁹ Finally, the temperature-dependent effects on the solvation dynamics of C153 and C151 are significant in TX-100 micelles and moderate in Brij-35

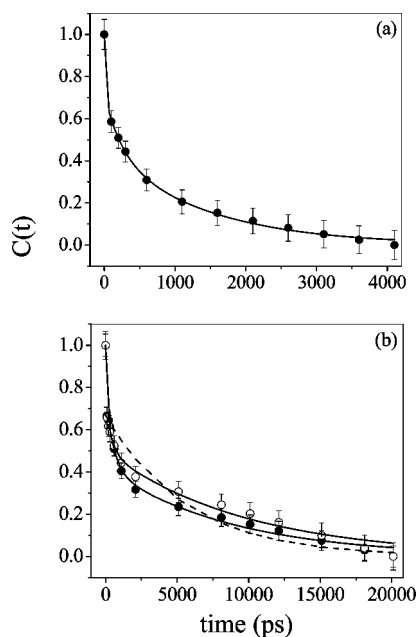


Figure 6. Solvation correlation functions for C153 in bulk $[(C_6)_3C_{14}P^+][Cl^-]$ (58 °C) with (a) 4 ns and (b) 20 ns full-scale time windows. This system serves as a model system in our study. Key: solid circles, purified $[(C_6)_3C_{14}P^+][Cl^-]$; open circles, unpurified $[(C_6)_3C_{14}P^+][Cl^-]$. The dashed line in panel b was constructed using the stretched exponential, $C(t) = 0.67[\exp(-t/2400 \text{ ps})]^{0.43}$, based upon the parameters obtained by Maroncelli and co-workers,¹¹ with the exception that the preexponential factor was normalized to our curves at the point at which the initial rapid component of solvation had been completed, namely, 100 ps. For purified $[(C_6)_3C_{14}P^+][Cl^-]$, $C(t)$ [4 ns] = $[0.28 \exp(-t/2.8 \text{ ps}) + 0.27 \exp(-t/240 \text{ ps}) + 0.45 \exp(-t/1420 \text{ ps})]$ and $C(t)$ [20 ns] = $[0.23 \exp(-t/2.5 \text{ ps}) + 0.35 \exp(-t/530 \text{ ps}) + 0.42 \exp(-t/8850 \text{ ps})]$. For unpurified $[(C_6)_3C_{14}P^+][Cl^-]$, $C(t)$ [20 ns] = $[0.28 \exp(-t/2.5 \text{ ps}) + 0.22 \exp(-t/410 \text{ ps}) + 0.50 \exp(-t/9710 \text{ ps})]$.

micelles.⁶⁰ In this work the authors emphasized the effect of micellar size and hydration on solvation dynamics in micellar media.

Phosphonium Ionic Liquids, their Properties, and the Construction of the Solvation Correlation Function, $C(t)$. Our results for the solvation dynamics of bulk $[(C_4)_3C_{16}P^+][Br^-]$ at 66 °C provide a solvation correlation function, $C(t)$, that has a component that is complete within 100 ps and that has a slower evolution over the course of a 20 ns time window. Such a result for a long-chain phosphonium halide ionic liquid is contrary to the report of Maroncelli and co-workers, who find that for $[(C_6)_3C_{14}P^+][Cl^-]$ essentially all of the solvation can be resolved, very little solvation has occurred by 100 ps, and the average solvation time is 6.7 ns¹¹ (Table 1). The authors attributed the slower dynamics to the presence of nonpolarizable longer alkyl chains in the ionic liquid.

This discrepancy led us to check the integrity of our experimental system by studying the solvation dynamics of $[(C_6)_3C_{14}P^+][Cl^-]$ ourselves as a control experiment. Our results were consistent with those obtained for $[(C_4)_3C_{16}P^+][Br^-]$; namely, there was a rapid component of solvation occurring within 100 ps, and the average solvation time was 3.9 ns, faster than that reported¹¹ (Table 1). From this result, we concluded that at least some of the observed differences could be attributed to sample quality. Considerable discussion has been given to the effect of impurities on the properties of ionic liquids.^{44,61,62} The role of water on the physical properties of ionic liquids is well-known, and an excellent study is provided by Bright and

TABLE 3: Zero-Time Spectral Parameters for C153 in $[(C_6)_3C_{14}P^+][Cl^-]$

spectral maximum ^a	nonpolar solvent ^b	$\nu^{("0")}$ ^a (cm^{-1})
$\nu_{\text{ex}} = 23\,590 \text{ cm}^{-1}$ ^c	hexane	20 710
$\nu_{\text{abs}} = 23\,430 \text{ cm}^{-1}$ ^{d,11}	hexane	20 560
$\nu_{\text{ex}} = 23\,590 \text{ cm}^{-1}$ ^c	2-methyl butane	20 630
$\nu_{\text{abs}} = 23\,430 \text{ cm}^{-1}$ ^{d,11}	2-methyl butane	20 420 ^e

^a Peak maxima of the excitation (ν_{ex}) (or absorption (ν_{abs})) and zero-time ($\nu^{("0")}$) spectra of C153 in $[(C_6)_3C_{14}P^+][Cl^-]$ obtained from log-normal fitting. The spectra of C153 in 2-methylbutane and $[(C_6)_3C_{14}P^+][Cl^-]$ were generously provided by Mark Maroncelli. Excitation spectra in our laboratory were collected at an emission wavelength of 600 nm. Unless otherwise indicated, the data were obtained with the purified phosphonium liquid. ^b Nonpolar solvent employed to obtain the excitation or absorption and emission spectra used for the construction of the zero-time spectrum. The $\nu_{\text{ex/abs}}$ and ν_{em} peak frequencies of C153 are very similar in hexane and 2-methylbutane. $\nu_{\text{ex}}(\text{hexane}) = 25\,710 \text{ cm}^{-1}$, $\nu_{\text{em}}(\text{hexane}) = 22\,370 \text{ cm}^{-1}$ and $\nu_{\text{abs}}(\text{2-methylbutane}) = 25\,700 \text{ cm}^{-1}$, $\nu_{\text{em}}(\text{2-methylbutane}) = 22\,300 \text{ cm}^{-1}$. ^c An excitation wavelength of 420 nm was used for the determination of the zero-time emission spectrum. ^d An excitation wavelength of 427 nm was used for the determination of the zero-time emission spectrum using an unpurified sample. ^e Zero-time emission maximum, $\nu^{("0")} = 20\,360 \text{ cm}^{-1}$, obtained by Maroncelli and co-workers.¹¹

co-workers.⁶² This work indicates that the solvation probe, PRODAN, is highly sensitive to water content. On the other hand, Ito et al.¹⁰ have shown that coumarin 153 is fortuitously insensitive to the presence of water, most likely owing to its hydrophobic character. In any case, the amount of water present in our sample (0.3% by weight, Table 1) provides only a minor perturbation in the results for PRODAN⁶² and thus is expected to have a negligible effect on C153, on the basis of the work of Ito et al.¹⁰

On the other hand, the $[(C_6)_3C_{14}P^+][Cl^-]$ we obtained from Cytec has a yellow tint and a viscosity of 230 cP at 58 °C. Maroncelli and co-workers obtained their sample from Cytec as well, reported similar sample properties, and performed their measurements with unpurified samples. Our purification procedure produces a colorless solvent with a viscosity of 80 cP at 58 °C (Table 1). The purified solvent is ~ 3 times less fluorescent than the unpurified solvent when excited at 420 nm at room temperature. The solvation dynamics, however, are not drastically different from those obtained with the unpurified liquid. We have seen a lengthening in the longer solvation component in the unpurified solvent compared to that in the purified one (see the caption to Figure 6 and Table 1), which is in accordance with the higher viscosity of the unpurified solvent.

While it is possible that some of these minor differences that we observe result from solvent purity and viscosity, there are, however, other more general factors that may explain the contrast between our results and those of Maroncelli and co-workers: namely, how $C(t)$ is computed. How accurately the solvation correlation function, $C(t)$, is constructed depends critically upon the quantities used in the denominator of eq 2. We have already indicated how sensitive the results can be to the choice of the time window used to collect the data, namely, the effect upon $\nu(\infty)$ or, more precisely, $\nu^{("∞")}$, but the determination of $\nu^{("0")}$ has its own idiosyncrasies. $\nu^{("0")}$ is the maximum of the estimated zero-time spectrum of the fluorescent probe after it has undergone intramolecular events contributing to its relaxation and before it has been altered by interactions with the solvent. The construction of the zero-time spectrum, which thus assumes such a time-scale separation of events, has been described by Fee and Maroncelli,⁴⁷ and we

TABLE 4: Comparison of Zero-Time Spectral Positions (cm⁻¹) Using Different Methods

system	$\nu(0),^a$ full peak	$\nu(0),^b$ approx peak	$\Delta\nu,^c$ full peak – approx peak	$\nu(0),^d$ approx mid	$\Delta\nu,^e$ full peak – approx mid	$\nu(0),^f$ full mid	$\Delta\nu,^g$ full mid – approx mid
[(C ₄) ₃ C ₁₆ P ⁺][Br ⁻] bulk, 66 °C	20 560	20 130	430	20 300	260	20 340	40
[(C ₄) ₃ C ₁₆ P ⁺][Br ⁻] micelle, room temperature	20 020	19 540	480	19 730	290	19 770	40
[(C ₄) ₃ C ₁₆ P ⁺][Br ⁻] micelle, 66 °C	20 200	19 650	550	19 910	290	19 950	40
[(C ₆) ₃ C ₁₄ P ⁺][Cl ⁻] bulk, purified, 58 °C	20 710	20 250	460	20 450	260	20 460	10
[(C ₆) ₃ C ₁₄ P ⁺][Cl ⁻] bulk, unpurified, 58 °C	20 550	20 080	470	20 230	320	20 240	10

^a Maximum of the zero-time spectrum obtained from log–normal fitting using the full Fee and Maroncelli procedure. ^b Maximum of the zero-time spectrum using the Fee and Maroncelli approximation, eq 3, where peak frequencies are employed. ^c Difference between the methods employing the full procedure and the approximation using peak frequencies. ^d Position of the zero-time spectrum using the Fee and Maroncelli approximation, eq 3, where midpoint frequencies are employed, $\nu_{\text{md}} = (\nu_+ + \nu_-)/2$, where ν_+ and ν_- are the midpoint frequencies at the blue and red edges of the spectrum, respectively. The midpoint values are recommended by Fee and Maroncelli.⁴⁷ ^e Difference between the methods employing the full procedure using peak maxima and the approximation using midpoint frequencies. ^f Midpoint position of the zero-time spectrum using the full Fee and Maroncelli procedure. ^g Difference between the methods employing the full procedure and the approximation using midpoint frequencies. The smaller deviation should not affect the value of the total Stokes shift and the nature of $C(t)$ significantly because in this case one should also consider the midpoint frequencies from the log–normal fits of different time-resolved spectra.

have shown that it is consistent with an independent method we have proposed, which compares the experimentally and theoretically determined reorganization energies in solvents over a wide range of polarities and indicates that 2068 cm⁻¹ of “solvation” in coumarin 153 is intramolecular.²⁴ This value is consistent with the reorganization energies obtained from the zero-time spectra cited in Table 1, which are ~1950 cm⁻¹.

To gain insight into the apparent discrepancy between our results and those of Maroncelli and co-workers,¹¹ we again considered the solvation of C153 in [(C₆)₃C₁₄P⁺][Cl⁻]. The required inputs for the calculation of the zero-time spectrum are the absorption (or excitation) spectrum of C153 in a nonpolar solvent and the corresponding spectrum in the polar solvent under investigation—in this case, the phosphonium ionic liquid. Also required is the emission spectrum of C153 in the nonpolar solvent. We used hexane as the nonpolar solvent to calculate the zero-time spectrum in polar solvents, while Maroncelli and co-workers used 2-methylbutane. Calculated zero-time peak frequencies using different spectra from different sources and obtained under different conditions are presented in Table 3. As indicated, the value of $\nu(0)$ is subject to the differences in the polar absorption/excitation spectra, the excitation wavelength, the nonpolar solvent, and even the fitting procedure used to obtain the spectral maximum. The data indicate that these factors can produce a difference of up to 350 cm⁻¹ in the position of the zero-time spectrum, which can represent ~20% of the total Stokes shift at 20 ns. Such factors must be taken into consideration when data are analyzed or results from different laboratories are compared. Ideally, the reorganization energy, λ , may be the best parameter to use for the computation of $C(t)$ because it is an integrated measure of the solvation dynamics (eq 1). The construction of λ , however, requires high-quality spectra, which are typically not provided by the traditional methods of spectral construction of 10–20 wavelength-resolved transients such as those illustrated in Figure 3.

We note, notwithstanding all the considerations enumerated above, that if the $C(t)$ of Maroncelli and co-workers is normalized to begin at the end of the rapid component we observe, then their $C(t)$ is within experimental error very similar to ours for both the purified and unpurified phosphonium liquid (Figure 6b and caption).

Finally, taking into consideration all of these issues, we believe that the full method of Fee and Maroncelli for obtaining the zero-time spectrum is the soundest available. The details of this method are clearly described in their paper,⁴⁷ are briefly alluded to above, and provide the basis for the construction of an *entire* emission spectrum. In this paper, Fee and Maroncelli

provide a simple equation for approximating the position of the zero-time spectrum:

$$\nu_{\text{em}}^{\text{P}}(0) = \nu_{\text{abs}}^{\text{P}} - (\nu_{\text{abs}}^{\text{nP}} - \nu_{\text{em}}^{\text{nP}}) \quad (3)$$

where P and nP refer to polar and nonpolar solvents, respectively. This approximate method has been employed by some workers, but we find that if it is successful in predicting the position of the zero-time spectrum, this success lies in using midpoint (rather than peak) frequencies in eq 3: $\nu_{\text{md}} = (\nu_+ + \nu_-)/2$, where ν_+ and ν_- are the midpoint frequencies at the blue and red edges of the spectrum, respectively. Also, to be consistent, this procedure recommends the use of midpoint frequencies in the construction of $C(t)$. The literature is often murky on these important details. We find that if midpoint frequencies are not employed, the approximation always provides a lower value (by at least a few hundred wavenumbers) for the peak maximum of the zero-time spectrum than the full method. We have illustrated this for the systems investigated here in Table 4, which provides a comparison of the positions of the zero-time spectrum for the solvents studied here using the rigorous method and the approximate method with peak and midpoint frequencies. Equation 3 is a quick and useful way of estimating the position of the zero-time spectrum,^{37,63} but we suggest that it is no substitute for using the full method—especially when quantitative interpretations of $C(t)$ are required.

For completeness, it has been suggested that the zero-time and steady-state frequencies could be obtained by rearranging eq 2 to

$$\nu(t) = C(t)[\nu(0) - \nu(\infty)] + \nu(\infty) \quad (4)$$

expressing $C(t)$ in terms of some function such as a sum of exponentials, using a curve-fitting procedure to extract the required parameters.^{64,65} We find that this procedure yields unphysical results (such as negative steady-state frequencies) if all parameters are permitted to vary. It always yields severely red-shifted zero-time spectra. We suggest that such a fitting procedure will not produce an accurate result unless the time resolution of the experiment is adequate for resolving most of the solvation response in the first place.

Conclusions

In studying a phosphonium ionic liquid that can form micelles in water, we conclude that our analysis of the comparable situation in an imidazolium liquid³⁶ is not as definitive as we had proposed: namely, that the majority of the early-time

solvation arises from the organic cation. Part of the difficulty in performing this analysis is most likely due to the amount of water that is associated with the micelle.

In the course of this work, we have found that the calculation of the solvation correlation function, $C(t)$, is surprisingly dependent upon the methods with which the zero-time spectrum is constructed. An interesting means of validating such spectral construction may ultimately be based upon computing $C(t)$ using dielectric spectra, as we have done elsewhere.²⁵ Finally, we have noted in another context, that of solvation by a protein environment,⁵⁷ how important an accurate computation of $C(t)$ is for the interpretation of the experimental results.

Acknowledgment. We thank Professor Mark Maroncelli for sharing his data for coumarin 153 in 2-methylbutane and in the phosphonium chloride and for helpful comments. We thank Professor Xueyu Song for helpful comments.

References and Notes

- (1) Seddon, K. R. *Nature (Materials)* **2003**, *2*, 363.
- (2) Anderson, J. L.; Ding, J.; Welton, T.; Armstrong, D. W. *J. Am. Chem. Soc.* **2002**, *124*, 14247.
- (3) Anderson, J. L.; Armstrong, D. W.; Wei, G.-T. *Anal. Chem.* **2006**, *78*, 2893.
- (4) Pandey, S. *Anal. Chim. Acta* **2006**, *556*, 38.
- (5) Karmakar, R.; Samanta, A. *J. Phys. Chem. A* **2002**, *106*, 6670.
- (6) Karmakar, R.; Samanta, A. *J. Phys. Chem. A* **2002**, *106*, 4447.
- (7) Karmakar, R.; Samanta, A. *J. Phys. Chem. A* **2003**, *107*, 7340.
- (8) Ingram, J. A.; Moog, R. S.; Ito, N.; Biswas, R.; Maroncelli, M. *J. Phys. Chem. B* **2003**, *107*, 5926.
- (9) Ito, N.; Arzhantsev, S.; Maroncelli, M. *Chem. Phys. Lett.* **2004**, *396*, 83.
- (10) Ito, N.; Arzhantsev, S.; Heitz, M.; Maroncelli, M. *J. Phys. Chem. B* **2004**, *108*, 5771.
- (11) Arzhantsev, S.; Ito, N.; Heitz, M.; Maroncelli, M. *Chem. Phys. Lett.* **2003**, *381*, 278.
- (12) Arzhantsev, S.; Hui, J.; Baker, G. A.; Naoki, I.; Maroncelli, M. Solvation dynamics in ionic liquids, results from ps and fs emission spectroscopy. Femtochemistry VII, 2005.
- (13) Arzhantsev, S.; Hui, J.; Naoki, I.; Maroncelli, M. *Chem. Phys. Lett.* **2006**, *417*, 524.
- (14) Hyun, B.-R.; Dzyuba, S. V.; Bartsch, R. A.; Quitevis, E. L. *J. Phys. Chem. A* **2002**, *106*, 7579.
- (15) Giraud, G.; Gordon, C. M.; Dunkin, I. R.; Wynne, K. *J. Chem. Phys.* **2003**, *119*, 464.
- (16) Cang, H.; Li, J.; Fayer, M. D. *J. Chem. Phys.* **2003**, *119*, 13017.
- (17) Shirota, H.; Funston, A. M.; Wishart, J. F.; Castner, E. W., Jr. *J. Chem. Phys.* **2005**, *122*, 184512.
- (18) Rajian, J. R.; Li, S.; Bartsch, R. A.; Quitevis, E. L. *Chem. Phys. Lett.* **2004**, *393*, 372.
- (19) Shirota, H.; Castner, E. W., Jr. *J. Phys. Chem. A* **2005**, *109*, 9388.
- (20) Weingärtner, H.; Knocks, A.; Schrader, W.; Kaatz, U. *J. Phys. Chem. A* **2001**, *105*, 8646.
- (21) Wakai, C.; Oleinikova, A.; Ott, M.; Weingärtner, H. *J. Phys. Chem. B* **2005**, *109*, 17028.
- (22) Ito, N.; Huang, W.; Richert, R. *J. Phys. Chem. B* **2006**, *110*, 4371.
- (23) Chowdhury, P. K.; Halder, M.; Sanders, L.; Calhoun, T.; Anderson, J. L.; Armstrong, D. W.; Song, X.; Petrich, J. W. *J. Phys. Chem. B* **2004**, *108*, 10245.
- (24) Headley, L. S.; Mukherjee, P.; Anderson, J. L.; Ding, R.; Halder, M.; Armstrong, D. W.; Song, X.; Petrich, J. W. *J. Phys. Chem. A* **2006**, *110*, 9549.
- (25) Halder, M.; Headley, L. S.; Mukherjee, P.; Song, X.; Petrich, J. W. *J. Phys. Chem. A* **2006**, *110*, 8623.
- (26) Margulis, C. J.; Stern, H. A.; Berne, B. J. *J. Phys. Chem. B* **2002**, *106*, 12017.
- (27) Shim, Y.; Duan, J.; Choi, M. Y.; Kim, H. J. *J. Chem. Phys.* **2003**, *119*, 6411.
- (28) Znamenskiy, V.; Kobrak, M. N. *J. Phys. Chem. B* **2004**, *108*, 1072.
- (29) Kobrak, M. N.; Znamenskiy, V. *Chem. Phys. Lett.* **2004**, *395*, 127.
- (30) Del Popolo, M. G.; Voth, G. A. *J. Phys. Chem. B* **2004**, *108*, 1744.
- (31) Morrow, T. I.; Maginn, E. J. *J. Phys. Chem. B* **2002**, *106*, 12807.
- (32) Hu, Z.; Margulis, C. J. *Proc. Natl. Acad. Sci. (U.S.A.)* **2006**, *103*, 831.
- (33) Lang, B.; Angulo, G.; Vauthey, E. *J. Phys. Chem. A* **2006**, *110*, 7028.
- (34) Samanta, A. *J. Phys. Chem. B* **2006**, *110*, 13704.
- (35) *J. Phys. Chem. B* **2007**, *111*, 4639–5029 (special issue).
- (36) Mukherjee, P.; Crank, J. A.; Halder, M.; Armstrong, D. W.; Petrich, J. W. *J. Phys. Chem. A* **2006**, *110*, 10725.
- (37) Adhikari, A.; Sahu, K.; Dey, S.; Ghosh, S.; Mandal, U.; Bhattacharyya, K. *J. Phys. Chem. B* **2007**, *111*, 12809.
- (38) Chakrabarty, D.; Seth, D.; Chakrabarty, A.; Sarkar, N. *J. Phys. Chem. B* **2005**, *109*, 5753.
- (39) Chakrabarty, A.; Seth, D.; Chakrabarty, D.; Setua, P.; Sarkar, N. *J. Phys. Chem. A* **2005**, *109*, 11110.
- (40) Seth, D.; Chakrabarty, A.; Setua, P.; Sarkar, N. *Langmuir* **2006**, *22*, 7768.
- (41) Seth, D.; Chakrabarty, A.; Setua, P.; Sarkar, N. *J. Phys. Chem. B* **2007**, *111*, 4781.
- (42) Gao, Y.; Li, N.; Zheng, L.; Bai, X.; Yu, L.; Zhao, X.; Zhang, J.; Zhao, M.; Li, Z. *J. Phys. Chem. B* **2007**, *111*, 2506.
- (43) Eastoe, J.; Gold, S.; Rogers, S. E.; Paul, A.; Welton, T.; Heenan, R. K.; Grillo, I. *J. Am. Chem. Soc.* **2005**, *127*, 7302.
- (44) Earle, M. J.; Gordon, C. M.; Plechkova, N. V.; Seddon, K. R.; Welton, T. *Anal. Chem.* **2007**, *79*, 758.
- (45) Turro, N. J.; Yekta, A. *J. Am. Chem. Soc.* **1978**, *100*, 5951.
- (46) Stam, J. v.; Depaemelaere, S.; De Schryver, F. C. *J. Chem. Educ.* **1998**, *75*, 93.
- (47) Fee, R. S.; Maroncelli, M. *Chem. Phys.* **1994**, *183*, 235.
- (48) Jimenez, R.; Fleming, G. R.; Kumar, P. V.; Maroncelli, M. *Nature* **1994**, *369*, 471.
- (49) Vajda, S.; Jimenez, R.; Rosenthal, S. J.; Fidler, V.; Fleming, G. R.; Castner, E. W., Jr. *J. Chem. Soc., Faraday Trans.* **1995**, *91*, 867.
- (50) Pal, S. K.; Peon, J.; Bagchi, B.; Zewail, A. H. *J. Phys. Chem. B* **2002**, *106*, 12376.
- (51) Nandi, N.; Bagchi, B. *J. Phys. Chem. B* **1997**, *101*, 10954.
- (52) Nandi, N.; Bagchi, B. *J. Phys. Chem. A* **1998**, *102*, 8217.
- (53) Nandi, N.; Bhattacharyya, K.; Bagchi, B. *Chem. Rev.* **2000**, *100*, 2013.
- (54) Bhattacharya, K. *Acc. Chem. Res.* **2003**, *36*, 95.
- (55) Pal, S. K.; Zewail, A. H. *Chem. Rev.* **2004**, *104*, 2099.
- (56) Ghosh, S.; Mandal, U.; Adhikari, A.; Dey, S.; Bhattacharya, K. *Int. Rev. Phys. Chem.* **2007**, *26*, 421.
- (57) Halder, M.; Mukherjee, P.; Bose, S.; Hargrove, M. S.; Song, X.; Petrich, J. W. *J. Chem. Phys.* **2007**, *127*, 055101.
- (58) Streletzky, K.; Phillies, G. D. *J. Langmuir* **1995**, *11*, 42.
- (59) Sen, P.; Mukherjee, S.; Halder, A.; Bhattacharyya, K. *Chem. Phys. Lett.* **2004**, *385*, 357.
- (60) Kumbhakar, M.; Goel, T.; Mukherjee, T.; Pal, H. *J. Phys. Chem. B* **2004**, *108*, 19246.
- (61) Seddon, K. R.; Stark, A.; Torres, M.-J. *Pure Appl. Chem.* **2000**, *72*, 2275.
- (62) Baker, S. N.; Baker, G. A.; Munson, C. A.; Chen, F.; Bukowski, E. J.; Cartwright, A. N.; Bright, F. V. *Ind. Eng. Chem. Res.* **2003**, *42*, 6457.
- (63) Sahu, K.; Mondal, S. K.; Ghosh, S.; Roy, D.; Sen, P.; Bhattacharyya, K. *J. Phys. Chem. B* **2006**, *110*, 1056.
- (64) Maroncelli, M.; Fleming, G. R. *J. Chem. Phys.* **1987**, *86*, 6221.
- (65) Horng, M. L.; Gardecki, J. A.; Papazyan, A.; Maroncelli, M. *J. Phys. Chem.* **1995**, *99*, 17311.
- (66) Bradaric, C. J.; Downard, A.; Kennedy, C.; Robertson, A. J.; Zhou, Y. *Green Chem.* **2003**, *5*, 143.
- (67) Eriksson, J. C.; Gillberg, G. *Acta Chem. Scand.* **1996**, *20*, 2019.
- (68) Weidemaier, K.; Tavernier, H. L.; Fayer, M. D. *J. Phys. Chem. B* **1997**, *101*, 9352.
- (69) Chakrabarty, A.; Chakrabarty, D.; Harza, P.; Seth, D.; Sarkar, N. *Chem. Phys. Lett.* **2003**, *382*, 508.
- (70) Kumbhakar, M.; Nath, S.; Mukherjee, T.; Pal, H. *J. Chem. Phys.* **2004**, *120*, 2824.